8154 *Inorg. Chem.* **2009**, *48*, 8154–8163
DOI: 10.1021/ic900285b

Inorganic Chemistry
Article

Oxygen Atom Transfer Reactions of Iridium and Osmium Complexes: Theoretical Study of Characteristic Features and Significantly Large Differences Between These Two Complexes

Atsushi Ishikawa,[†] Yoshihide Nakao,[†] Hirofumi Sato,[†] and Shigeyoshi Sakaki*[,†,‡]

[†]*Department of Molecular Engineering, Graduate School of Engineering, Kyoto University, Nishikyo-ku, Kyoto 615-8510, Japan, and* [‡]*Fukui Institute for Fundamental Chemistry, Kyoto University, Nishi-hiraki cho, Takano, Sakyo-ku, Kyoto 606-8301, Japan*

Received February 11, 2009

Oxygen atom transfer reaction between ML_3═O and ML_3 (L = 2,4,6-trimethylphenyl (Mes) for M = Ir and L = 2,6-diisopropylphenylimide (NAr) for M=Os) was theoretically investigated by DFT method. The optimized geometry of $(Mes)_3Ir-O-Ir(Mes)_3$ agrees well with the experimental one, although those of $(CH_3)_3Ir-O-Ir(CH_3)_3$ and $Ph_3Ir-O-IrPh_3$ are much different from the experimental one of the Mes complex. These results indicate that the bulky ligand plays important roles to determine geometry of the μ-oxo dinuclear Ir complex. Theoretical study of the real systems presents clear pictures of these oxygen atom transfer reactions, as follows: In the Ir reaction system, (i) the μ-oxo bridged dinuclear complex is more stable than the infinite separation system in potential energy surface, indicating this is incomplete oxygen atom transfer reaction which does not occur at very low temperature, (ii) unsymmetrical transition state is newly found, in which one Ir−O distance is longer than the other one, (iii) unsymmetrical local minimum is also newly found between the transition state and the infinite separation system, and (iv) activation barrier (E_a) is very small. In the Os reaction system, (v) the transition state is symmetrical, while no intermediate is observed unlike the Ir reaction system, and (vi) E_a is very large. These results are consistent with the experimental results that the reaction rapidly occurs in the Ir system but very slowly in the Os system, and that the μ-oxo bridged dinuclear intermediate is detected in the Ir system but not in the Os system. To elucidate the reasons of these differences between Ir and Os systems, the E_a value is decomposed into the nuclear and electronic factors. The former is the energy necessary to distort ML_3 and ML_3═O moieties from their equilibrium geometries to those in the transition state. The latter depends on donor−acceptor interaction between ML_3═O and ML_3. The nuclear factor is much larger in the Os system than in the Ir system and it contributes to about 70% of the difference in E_a. The energy gap between the donor orbital of ML_3 and the acceptor orbital of ML_3═O is much larger in the Os system than in the Ir system, which also contributes to the lower E_a value of the Ir system than that of the Os system.

Introduction

Oxygen atom transfer reactions mediated by transition metal complexes (eq 1) are of considerable interest in synthetic and biomimetic chemistries.[1−3]

$$M - O + R \rightarrow M + O - R \qquad (1)$$

Because the oxygen atom is removed from metal center and added to substrate as shown in eq 1, this reaction deeply relates to catalytic oxygenation processes such as olefin epoxidation[4−6] and hydroxylation.[7−10] This process is also important in biological systems; actually a number of important metalloenzymes mediate atom transfer reaction as key step.[11,12] One of the typical examples is cytochrome P-450 class of enzymes.[13−16] Also, oxygen atom transfer reactions

*To whom correspondence should be addressed. E-mail: sakaki@moleng.kyoto-u.ac.jp.

(1) Holm, R. H. *Chem. Rev.* **1987**, *87*, 1401.
(2) Woo, L. K. *Chem. Rev.* **1993**, *93*, 1125.
(3) Shilov, A. E.; Shteinman, A. A. *Acc. Chem. Res.* **1999**, *32*, 763.
(4) Hess, J. S.; Leelasubcharoen, S.; Rheingold, A. L.; Doren, D. J.; Theopold, K. H. *J. Am. Chem. Soc.* **2002**, *124*, 2454.
(5) Merkx, M.; Kopp, D. A.; Sazinsky, M. H.; Blazyk, J. L.; Muller, J.; Lippard, S. J. *Angew. Chem., Int. Ed.* **2001**, *40*, 2782.
(6) Dobler, C.; Mehltretter, G.; Beller, M. *Angew. Chem., Int. Ed.* **1999**, *38*, 3026.
(7) Kolb, H. C.; VanNieuwenhze, M. S.; Sharpless, K. B. *Chem. Rev.* **1994**, *94*, 2483.
(8) Andersson, M. A.; Epple, R.; Fokin, V. V.; Sharpless, K. B. *Angew. Chem., Int. Ed.* **2002**, *41*, 472.
(9) Chen, K.; Costas, M.; Kim, J.; Tipton, A. K.; Que, L., Jr. *J. Am. Chem. Soc.* **2002**, *124*, 3026.
(10) Ryu, J. Y.; Kim, J.; Costas, M.; Chen, K.; Nam, W.; Que, L., Jr. *Chem. Commun.* **2002**, 1288.
(11) Holm, R. H.; Kennepohl, P.; Solomon, E. I. *Chem. Rev.* **1996**, *96*, 2239.
(12) Ostovic, D.; Bruice, T. C. *Acc. Chem. Res.* **1992**, *25*, 314.
(13) de Visser, S. P.; Ogliaro, F.; Sharma, P. K.; Shaik, S. *Angew. Chem., Int. Ed.* **2002**, *41*, 1947.

 Published on Web 08/11/2009

Scheme 1. Molecular Structures of Iridium and Osmium Complexes[a]

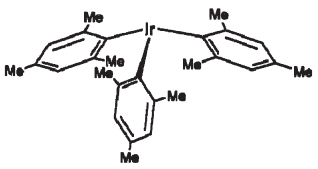

(A) Trimesityliridium (**Ir(Mes)$_3$**)

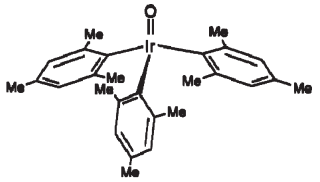

(B) Oxotrimesityliridium (**Ir(Mes)$_3$=O**)

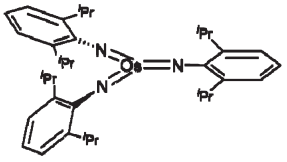

(C) Tris(2,6-diisopropylphenylimide)osmium (**Os(NAr)$_3$**)

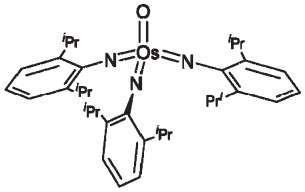

(D) Oxo-tris(2,6-diisopropylphenylimide)osmium(**Os(NAr)$_3$=O**)

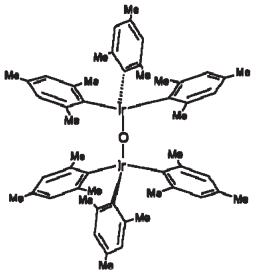

(E) μ-oxohexamesityldiiririum (**IM$_{IrMes}$**) :(Mes)$_3$Ir-O-Ir(Mes)$_3$

[a] (A) Trimesityliridium (**Ir(Mes)$_3$**), (B) Oxotrimesityliridium (**Ir(Mes)$_3$=O**), (C) Tris(2,6-diisopropylphenylimide)osmium (**Os(NAr)$_3$**), (D) Oxo-tris-(2,6-diisopropylphenylimide)osmium (**Os(NAr)$_3$=O**), (E) μ-oxohexamesityldiiririum (**IM$_{IrMes}$**): (Mes)3Ir−O−Ir(Mes)$_3$.

between nonheme iron-oxo and iron complexes are reported.[17−20] Another important example is activation of dioxygen molecule,[4−6] in which the O−O bond cleavage occurs and one of the two oxygen atoms is utilized for oxidation reaction via oxygen-atom transfer reaction.

To utilize effectively the oxygen atom transfer reaction in catalytic, biomimetic, and biological chemistries, correct knowledge of this reaction such as transition state geometry, its electronic structure, and determining factor of reactivity is indispensable. In this regard, several experimental and theoretical studies have been carried out to present such knowledge and clarify the determining factors so far.[17−24]

Recently, the oxygen atom transfer reactions between late transition metal complexes and their oxo-complexes (Scheme 1A−D) were investigated experimentally and theoretically by Fortner et al. and several interesting results were reported,[25] as follows; the oxygen atom transfer between trimesityliridium(III) complex **Ir(Mes)$_3$** (Mes = 2,4,6-trimethylphenyl) and its oxo-complex **Ir(Mes)$_3$=O** very rapidly occurs, while that between similar tris(2,6-diisopropylphenyl)imide osmium(V) complex **Os(NAr)$_3$** (Ar = 2,6-diisopropylphenyl) and its oxo-complex **Os(NAr)$_3$=O** very slowly occurs; the rate constant is 5×10^7 M^{-1} s^{-1} at 20 °C for the former reaction but 1.8×10^{-5} M^{-1} s^{-1} for the latter reaction. This significantly large difference cannot be understood from thermodynamic point of view, since the Ir=O bond energy is little different from the Os=O bond energy by only 0.86 kcal/mol.[26] Also, another interesting result was reported about the reaction behavior, as follows; Because the oxygen atom is transferred from one metal complex to the other one, it is likely that the transition state takes μ-oxo bridged dinuclear geometry. Interestingly, such μ-oxo bridged dinuclear complex (**Mes)$_3$Ir−O−Ir(Mes)$_3$** (**IM$_{IrMes}$**, see Scheme 1) was isolated in the reaction of the iridium system and analyzed by the X-ray crystallography.[25] The linear μ-oxo bridged dinuclear complex was also spectroscopically observed in the reaction of the iridium system below −80 °C.[25] Because of the formation of the μ-oxo bridged

(14) de Visser, S. P.; Ogliaro, F.; Harris, N.; Shaik, S. *J. Am. Chem. Soc.* **2001**, *123*, 3037.
(15) de Visser, S. P.; Ogliaro, F.; Sharma, P. K.; Shaik, S. *J. Am. Chem. Soc.* **2002**, *124*, 11809.
(16) Ogliaro, F.; Harris, N.; Cohen, S.; Filatov, M.; de Visser, S. P.; Shaik, S. *J. Am. Chem. Soc.* **2000**, *122*, 8977.
(17) Brown, S. N.; Mayer, J. M. *Inorg. Chem.* **1992**, *31*, 4091.
(18) Gangopadhyay, J.; Sengupta, S.; Bhattacharyya, S.; Chakraborty, I.; Chakravorty, A. *Inorg. Chem.* **2002**, *41*, 2616.
(19) Sastri, C. V.; Oh, K.; Lee, Y. J.; Seo, M. S.; Shin, W.; Nam, W. *Angew. Chem., Int. Ed.* **2006**, *45*, 3992.
(20) de Visser, S. P.; Lee, Y.-M.; Nam, W. *Eur. J. Inorg. Chem.* **2008**, 1027.
(21) Matsuda, T.; Tanaka, K.; Tanaka, T. *Inorg. Chem.* **1979**, *18*, 454.
(22) Seymore, S. B.; Brown, S. N. *Inorg. Chem.* **2000**, *39*, 325.
(23) Veige, A. S.; Slaughter, L. M.; Lobkovsky, E. B.; Wolczanski, P. T.; Matsunaga, N.; Decker, S. A.; Cundari, T. R. *Inorg. Chem.* **2003**, *42*, 6204.
(24) Pietsch, M. A.; Hall, M. B. *Inorg. Chem.* **1996**, *35*, 1273.
(25) Fortner, K. C.; Laitar, D. S.; Muldoon, J.; Pu, L. H.; Braun-Sand, S. B.; Wiest, O.; Brown, S. N. *J. Am. Chem. Soc.* **2007**, *129*, 588.
(26) We theoretically evaluated Ir = O bond energy of **Ir(CH$_3$)$_3$ = O** and Os = O bond energy of **Os(NCH$_3$)$_3$ = O** with various methods; see Supporting Information, Table S3. Theoretically evaluated difference between the Ir=O and Os=O bond energies does not agree with experimental difference (0.84 kcal/mol). Further investigation is necessary for this issue.

dinuclear complex, this reaction is experimentally understood to be "incomplete" oxygen atom transfer reaction.[1] This incomplete oxygen atom transfer reaction changes to a "complete" oxygen atom transfer reaction at higher temperature. On the other hand, such μ-oxo dinuclear intermediate has been neither isolated nor detected in the osmium reaction system. It is of considerable interest to characterize reaction features of these iridium and osmium complexes including the transition state and the intermediate, and to elucidate the reasons why the oxygen atom transfer reaction rapidly occurs in the iridium system but very slowly in the osmium system[25] despite of their similar geometries and M=O bond energies.[26] Forter et.al. also theoretically investigated these reactions and presented fundamental explanation on differences in reorganization energy and frontier orbitals based on DFT computational results of model systems.

In this paper, we wish to report theoretical study of above-described oxygen atom transfer reaction between **Ir(Mes)$_3$** and **Ir(Mes)$_3$=O** and that between **Os(NAr)$_3$** and **Os(NAr)$_3$=O**. Our purposes here are to elucidate the reaction features, to make clear comparison between the reactions of iridium and osmium complexes, and to provide the clear understanding for the reasons of the significantly large differences between these two reaction systems. We wish to emphasize that unsymmetrical transition state and intermediate are newly found in the iridium reaction system. We believe that these theoretical results are valuable for designing efficient atom transfer reaction and making further development of this type of reaction.

Computational Methods

All these **Ir(Mes)$_3$**, **Ir(Mes)$_3$=O**, **Os(NAr)$_3$**, and **Os(NAr)$_3$=O** are experimentally reported to be neutral.[37,39] For all compounds, the singlet state was calculated to be the most stable; see Table S2 in Supporting Information.

We employed real complexes and their small models in calculations. In model complexes, the mesityl groups of the iridium complexes and the 2, 6-diisopropylphenyl groups of the osmium complexes were replaced by methyl groups. These trimethyl iridium and osmium complexes and their oxo complexes are represented by **Ir(CH$_3$)$_3$**, **Os(NCH$_3$)$_3$**, **Ir(CH$_3$)$_3$=O**, and **Os(NCH$_3$)$_3$=O**, respectively. All these model complexes are neutral and their ground states are singlet, too.

In both model and real systems, we optimized geometries and evaluated energy changes with the density functional theory (DFT) using B3LYP functional.[27,28] In model systems, two basis set systems (BS-I and BS-II) were employed for calculation. In BS-I, Stuttgart-Dresden-Bonn effective core potentials (ECPs) were used to replace core electrons of iridium and osmium atoms, and (311111/22111/411) basis sets were used for their valence electrons.[29] Usual 6-31G (d) basis sets[30] were used for carbon, oxygen, nitrogen, and hydrogen atoms. In BS-II, Dunning cc-pVDZ basis sets[31] were used for carbon, nitrogen, oxygen, and hydrogen atoms, while the same basis sets and ECPs as those of BS-I were employed for the metal atoms. BS-I was used for geometry optimization and calculation of vibrational frequency and BS-II was used for evaluation of energy changes.

In the real systems, moderately smaller basis set systems (BS-III and BS-IV) were employed: In BS-III, Los Alamos ECPs and (341/321/21) basis sets were used for core and valence electrons of metal atoms,[32] respectively. Usual 6-31G(d) basis sets were used for oxygen and nitrogen atoms of imide group, and 6-31G for carbon and hydrogen atoms of phenyl ring. STO-3G basis sets were used for methyl group of mesityl ligand and isopropyl group of imide ligand. The BS-III was used for geometry optimization and evaluation of vibrational frequency. BS-IV was almost the same as BS-I, while d polarization function was deleted from carbon atom of methyl and isopropyl groups to save CPU time. Zero-point energy was evaluated with the DFT/BS-III method under assumption of harmonic oscillator.

Solvation effects of dichloromethane and benzene were evaluated with PCM method,[33] where the geometries were reoptimized in solution with the PCM method at the DFT/BS-III level. All the computations were performed by Gaussian 03 program package.[34]

In this oxygen atom transfer reaction, the transition state and intermediate are formed as adduct of ML_3 and ML_3=O (M = Ir or Os; L = Mes or NAr). Because the entropy of reactants considerably decreases in this process, we must present discussion based on the Gibbs free energy change, ΔG^0. Though the ΔG^0 value is evaluated in gas phase by Gaussian 03 program, the ΔG^0 value in solution is much different from that in gas phase because translation movement is considerably suppressed in solution and hence the translation entropy is much smaller than that in gas phase. Here, we evaluated the translational entropy in solution by considering free space available for the translation movement, according to the method proposed by Whitesides et al.[35] The molecular volume of solvent is estimated by DFT/BS-I-calculated electronic density; see Supporting Information page S4 for the details.

Results

Preliminary Investigation with Model Systems, Ir(CH$_3$)$_3$, Ir(CH$_3$)$_3$=O, Os(NCH$_3$)$_3$, and Os(NCH$_3$)$_3$=O. Both **Ir(CH$_3$)$_3$** and **Ir(CH$_3$)$_3$=O** have tetrahedral-like structures with C_{3v} symmetry, which agree well with their experimental structures of the real complexes, as shown in Figure 1.[36,37] On the other hand, **Os(NCH$_3$)$_3$** has trigonal planar structure with D_{3h} symmetry unlike **Ir(CH$_3$)$_3$**, while **Os(NCH$_3$)$_3$=O** has tetrahedral-like structure with

(27) Becke, A. D. *J. Chem. Phys.* **1993**, *98*, 5648.
(28) (a) Lee, C.; Yang, W.; Parr, R. G. *Phys. Rev. B* **1988**, *37*, 785. (b) Miehlich, B.; Savin, A.; Stoll, H.; Preuss, H. *Chem. Phys. Lett.* **1989**, *157*, 200.
(29) Andrae, D.; Haussermann, U.; Dolg, M.; Stoll, H.; Preuss, H. *Theor. Chem. Acta.* **1990**, *77*, 123.
(30) Ditchfield, R.; Hehre, W. J.; Pople, J. A. *J. Chem. Phys.* **1971**, *54*, 724.
(31) Dunning, T. H., Jr. *J. Chem. Phys.* **1989**, *90*, 1007.
(32) Hay, P. J.; Wadt, W. R. *J. Chem. Phys.* **1985**, *82*, 299.
(33) Miertus, S; Scrocco, E.; Tomasi, J. *Chem. Phys.* **1981**, *55*, 117.
(34) Frisch, M. J.; Trucks, G. W.; Schlegel, H. B.; Scuseria, G. E.; Robb, M. A.; Cheeseman, J. R.; Montgomery, J. A., Jr.; Vreven, T.; Kudin, K. N.; Burant, J. C.; Millam, J. M.; Iyengar, S. S.; Tomasi, J.; Barone, V.; Mennucci, B.; Cossi, M.; Scalmani, G.; Rega, N.; Petersson, G. A.; Nakatsuji, H.; Hada, M.; Ehara, M.; Toyota, K.; Fukuda, R.; Hasegawa, J.; Ishida, M.; Nakajima, T.; Honda, Y.; Kitao, O.; Nakai, H.; Klene, M.; Li, X.; Knox, J. E.; Hratchian, H. P.; Cross, J. B.; Bakken, V.; Adamo, C.; Jaramillo, J.; Gomperts, R.; Stratmann, R. E.; Yazyev, O.; Austin, A. J.; Cammi, R.; Pomelli, C.; Ochterski, J. W.; Ayala, P. Y.; Morokuma, K.; Voth, G. A.; Salvador, P.; Dannenberg, J. J.; Zakrzewski, V. G.; Dapprich, S.; Daniels, A. D.; Strain, M. C.; Farkas, O.; Malick, D. K.; Rabuck, A. D.; Raghavachari, K.; Foresman, J. B.; Ortiz, J. V.; Cui, Q.; Baboul, A. G.; Clifford, S.; Cioslowski, J.; Stefanov, B. B.; Liu, G.; Liashenko, A.; Piskorz, P.; Komaromi, I.; Martin, R. L.; Fox, D. J.; Keith, T.; Al-Laham, M. A.; Peng, C. Y.; Nanayakkara, A.; Challacombe, M.; Gill, P. M. W.; Johnson, B.; Chen, W.; Wong, M. W.; Gonzalez, C.; Pople, J. A. *Gaussian 03*, revision D.02; Gaussian, Inc.: Wallingford, CT, 2004.
(35) Mammen, M.; Shakhnovich, E. I.; Deutch, J. M.; Whitesides, G. M. *J. Org. Chem.* **1998**, *63*, 3821.
(36) Hay-Motherwell, R. S.; Wilkinson, G; Hussain-Bates, B.; Hursthouse, M. B. *J. Chem. Soc., Dalton Trans.* **1992**, 3477.
(37) Hay-Motherwell, R. S.; Wilkinson, G; Hussain-Bates, B.; Hursthouse, M. B. *Polyhedron* **1993**, *12*, 2009.

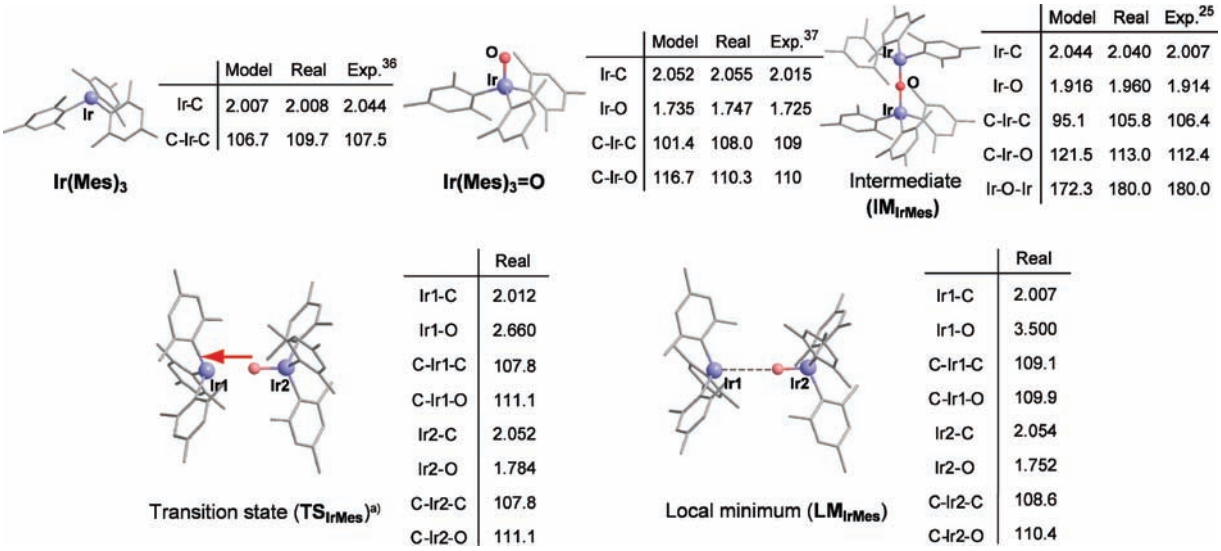

Figure 1. Selected bond lengths (in Å) and angles (in degree) of the iridium reaction system where hydrogen atoms are omitted. (a) The displacement vector corresponding to imaginary frequency is shown by arrow.

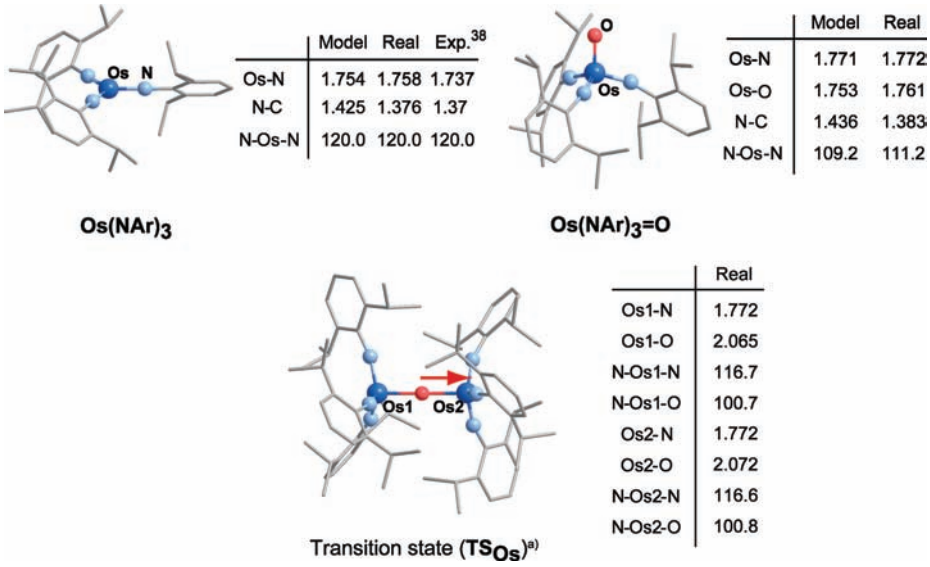

Figure 2. Selected bond lengths (in Å) and angles (in degree) of the osmium reaction system where hydrogen atoms are omitted. (a) The displacement vector corresponding to imaginary frequency is shown by arrow.

C_{3v} symmetry like $\mathbf{Ir(CH_3)_3{=}O}$. These geometries also agree well with the experimental structures of the real complexes except for the Os−N−Me angle (Figure 2);[38] the optimized Os−N−Me angle is 157°, whereas it is linear in the experimental structure. The bending geometry was reported in previous computational study of similar small model.[39] In further smaller model, $Os(NH)_3$, the optimized Os−N−H angle (134°) becomes much smaller. From these results, it is concluded that the Os−N-R bending geometry is favorable from the viewpoint of electronic structure but bulky substituent leads to the formation of the linear geometry. In the later half of this work, we employed a real substituent.

In the iridium system, we optimized the μ-oxo bridged dinuclear complex, $(CH_3)_3$−Ir−O−Ir−$(CH_3)_3$, $\mathbf{IM_{IrMe}}$. The optimized geometry of $\mathbf{IM_{IrMe}}$ agrees well with the experimental geometry except for too small C−Ir−O and C−Ir−C angles, as shown in Figure 1. These small angles are easily interpreted in terms of much smaller methyl group than mesityl group. This result again indicates that the electronic factor favors this bending geometry and the bulky substituent is necessary for the linear geometry. $\mathbf{IM_{IrMe}}$ is calculated to be more stable than the infinite separation system by 18.2 kcal/mol with the DFT/BS-II method. This computational result of the iridium model system suggests that the oxygen atom transfer reaction of the iridium system is "incomplete".

In the osmium system, the transition state could not be optimized. Instead of the transition state, the μ-oxo dinuclear complex $(CH_3N)_3Os{-}O{-}Os(NCH_3)_3$ was optimized unexpectedly, in which the Os−O−Os moiety is

(38) Anhaus, J. T.; Kee, T. P.; Schofield, M. H.; Schrock, R. R. *J. Am. Chem. Soc.* **1990**, *112*, 1642.
(39) Schofield, M. H.; Kee, T. P.; Anhaus, J. T.; Schrock, R. R.; Johnson, K. H.; Davis, W. M. *Inorg. Chem.* **1991**, *30*, 3595.

Table 1. Relative Values of Calculated Thermodynamic Parameters (kcal/mol) for Ir and Os Real Systems in Gas Phase

		Ir system				Os system	
	temperature/K	$\mathbf{IM_{IrMes}}$	$\mathbf{TS_{IrMes}}$	$\mathbf{LM_{IrMes}}$	$\mathbf{Ir(Mes)_3 + Ir(Mes)_3{=}O}$	$\mathbf{TS_{Os}}$	$\mathbf{Os(NAr)_3 + Os(NAr)_3{=}O}$
electronic energy (e_0)		−4.2	−2.1	−3.2	0.0	33.6	0.0
e_0 + zero point energy		−3.9	−1.9	−4.1	0.0	33.3	0.0
e_0 + zero point energy + thermal energy	50	−4.0	−2.0	−3.8	0.0	33.2	0.0
	100	−3.9	−1.9	−3.6	0.0	33.2	0.0
	298.15	−2.9	−1.2	−2.8	0.0	34.5	0.0
thermal enthalpy	50	−4.1	−2.1	−3.9	0.0	33.2	0.0
	100	−4.1	−2.1	−3.8	0.0	33.0	0.0
	298.15	−3.5	−1.8	−3.4	0.0	33.9	0.0
Gibbs free energy	50	−1.2	0.7	−2.3	0.0	33.3	0.0
	100	1.5	3.2	−0.3	0.0	39.8	0.0
	298.15	12.4	13.6	8.0	0.0	52.6	0.0

bent like $\mathbf{IM_{IrMe}}$. This geometry possesses no imaginary frequency. We optimized the linear μ-oxo dinuclear osmium complex under constraint of the linear Os−O−Os moiety. However, it exhibits imaginary frequency of about $49.8i\ \mathrm{cm}^{-1}$, which mainly involves the Os−O−Os bending motion. Moreover, the linear structure is much less stable than the bent structure by 44.4 kcal/mol. These results lead to conclusions that this linear μ-oxo dinuclear osmium complex is not the proper transition state for the oxygen atom transfer reaction, and that the transition state cannot be successfully optimized with the model system.

It is likely that the above problems observed in both iridium and osmium model systems arise from the oversimplification of the ligand. The importance of the bulky ligand for the oxygen atom transfer reaction was also experimentally suggested.[40] Thus, the real system should be employed for theoretical study to present the correct understanding of the oxygen atom transfer reaction.

Geometries of Reactant, Intermediate, and Transition States of Real Systems. Optimized geometries of $\mathbf{Ir(Mes)_3}$, $\mathbf{Ir(Mes)_3{=}O}$, and intermediate $\mathbf{IM_{IrMes}}$ agree well with their experimental ones,[25,36,37] as shown in Figure 1. $\mathbf{IM_{IrMes}}$ possesses no imaginary frequency, indicating that this is equilibrium structure. It is noted that the Ir−O−Ir moiety is linear in $\mathbf{IM_{IrMes}}$ unlike that of $\mathbf{IM_{IrMe}}$. We carried out geometry optimization of other model systems, $\mathbf{Ir(Ph)_3}$ and $\mathbf{Ir(Ph)_3{=}O}$, in which mesityl groups were substituted for phenyl groups. In this model, the μ-oxo bridged Ir−O−Ir moiety is bending unlike the real system, although the potential energy surface is flat; see Supporting Information Figures S1 and S2. Thus, it should be concluded that the mesityl groups play important roles to determine the geometry of the intermediate; in other words, the geometry of the μ-oxo bridged dinuclear iridium intermediate is determined by delicate balance between electronic and steric factors. The transition state ($\mathbf{TS_{IrMes}}$) was newly optimized in this work. It has unsymmetrical μ-oxo bridged dinuclear geometry in which one Ir−O distance is 1.784 Å and the other one is 2.660 Å, as shown in Figure 1. This transition state exhibits only one imaginary frequency, in which the oxygen atom is moving from one iridium center toward the other center. Besides this transition state and the symmetrical μ-oxo bridged dinuclear intermediate, we found the unsymmetrical local energy minimum ($\mathbf{LM_{IrMes}}$) in which one Ir−O distance is 1.752 Å and the other one is 3.500 Å, as shown in Figure 1.

In the osmium real system, the optimized geometry of $\mathbf{Os(NAr)_3}$ also agrees well with its experimental structure,[25] as shown in Figure 2. Optimized transition state ($\mathbf{TS_{Os}}$) is symmetrical. It possesses one imaginary frequency, in which the oxygen atom is moving from one osmium center toward the other osmium center, too.

It is noted that the serious disagreements between the optimized geometries of small models and the experimental ones disappear in the optimized geometries of real systems; for instance, the Os−N−C moiety is bending in $\mathbf{Os(NCH_3)_3}$ but becomes almost linear in $\mathbf{Os(NAr)_3}$, and the Ir−O−Ir moiety is bending $\mathbf{IM_{IrMe}}$ but becomes almost linear in $\mathbf{IM_{IrMes}}$.

Potential Energy Curves (PECs) of the Oxygen Atom Transfer Reaction. The PEC of the real system is evaluated against one M−O distance, where the other moiety was optimized without any constraint. Potential and Gibbs free energies were calculated for important molecular structures such as two intermediates and transition state are shown in Table 1. It is noted that the μ-oxo dinuclear intermediate ($\mathbf{IM_{IrMes}}$) is more stable than both the local minimum ($\mathbf{LM_{IrMes}}$) and the infinite separation system. The activation barrier of this reaction is quite small (3.9 kcal/mol).[41] Thus, the presence of the stable $\mathbf{IM_{IrMes}}$ indicates that the oxygen atom transfer reaction does not occur at low temperature.

Entropy effect should be considered to discuss the reaction. In gas phase, the Gibbs free energy change (ΔG^0) of $\mathbf{IM_{IrMes}}$ is much larger (12.4 kcal/mol) than that of the infinite separation system at 298.15 K, but it decreases to 1.5 kcal/mol at 100 K and −1.2 kcal/mol at 50 K. The $\Delta G^{0\ddagger}$ value is 0.7 kcal/mol at 50 K and 13.6 kcal/mol at 298.15 K.[41]

In solvent, we need to correct ΔG^0 value because translation movement is considerably suppressed in solution and

(40) William, D. S.; Schrock, R. R. *Organometallics* **1963**, *12*, 1148.

(41) In iridium system, the activation barrier in the potential energy surface is defined as the zero-point corrected energy difference between the infinite separation system and the intermediate ($\mathbf{IM_{IrMes}}$), because the transition state is more stable than the infinite separation system. On the other hand, the activation barrier in the free energy surface ($\Delta G^{0\ddagger}$) is defined as the energy difference between the transition state and the infinite separation system because the intermediate is less stable that the infinite separation system in the free energy surface.

Table 2. Relative Values of Calculated Thermodynamic Parameters (kcal/mol) for Ir and Os Real Systems in Solution [a] Where the Translational Entropy Was Corrected by Whitesides' Method[35]

		Ir system (in dichloromethane)				Os system (in benzene)	
	temperature/K	$\mathbf{IM_{IrMes}}$	$\mathbf{TS_{IrMes}}$	$\mathbf{LM_{IrMes}}$	$\mathbf{Ir(Mes)_3 + Ir(Mes)_3{=}O}$	TS_{Os}	$\mathbf{Os(NAr)_3 + Os(NAr)_3{=}O}$
electronic energy (E_0)		−3.9	0.5	−0.2	0.0	31.2	0.0
E_0 + zero point energy		−3.0	1.0	−0.7	0.0	30.3	0.0
E_0 + zero point energy + thermal energy	50	−3.1	1.0	−0.6	0.0	30.3	0.0
	100	−3.0	1.1	−0.3	0.0	30.3	0.0
	298.15	−2.1	1.7	0.5	0.0	31.3	0.0
thermal enthalpy	50	−3.2	0.9	−0.7	0.0	30.1	0.0
	100	−3.2	0.9	−0.5	0.0	30.1	0.0
	298.15	−2.7	1.1	−0.1	0.0	30.7	0.0
Gibbs free energy	50	−0.5	3.4	1.4	0.0	33.2	0.0
	100	2.2	5.9	3.4	0.0	36.3	0.0
	298.15	12.6	15.9	10.9	0.0	48.3	0.0
corrected Gibbs free energy	50	−1.0	2.9	0.9	0.0	32.6	0.0
	100	1.4	5.2	2.7	0.0	35.0	0.0
	298.15	8.8	12.1	7.1	0.0	43.8	0.0

[a] Geometry optimization and energy evaluation were carried out by the PCM method at B3LYP/BS-III and BS3LYP/BS-IV levels, respectively.

Scheme 2. Definition of the Pendant Angle

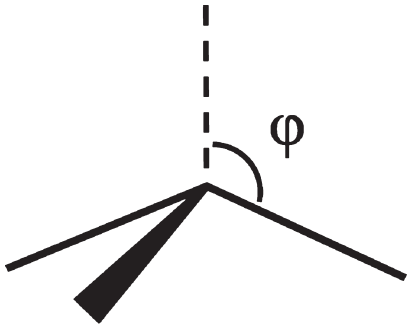

the translation entropy is much smaller than that in gas phase. We employed here the method proposed by Whitesides et.al.[35] to evaluate entropy in solution. Evaluated ΔG^0 value of $\mathbf{IM_{IrMes}}$ is −1.0 kcal/mol at 50 K, 1.4 kcal/mol at 100 K, and 8.8 kcal/mol at 298.15 K. The $\Delta G^{0\ddagger}$ value is 2.9 kcal/mol at 50 K, 5.2 kcal/mol at 100 K, and 12.1 kcal/mol at 298.15 K, as shown in Table 2. These computational results are consistent with the experimental fact that $\mathbf{IM_{IrMes}}$ is isolated at 100 K, but the oxygen atom transfer reaction occurs at higher temperature.

On the other hand, no intermediate is observed in the osmium system, in which only transition state ($\mathbf{TS_{Os}}$) was optimized, as shown in Figure 2. It is noted that the activation barrier is very large. The $\Delta G^{0\ddagger}$ value was evaluated to be 35.0 kcal/mol at 100 K and 43.8 kcal/mol at 298.15 K as shown in Table 2. These computational results reproduce well that the reaction behavior is completely different between iridium and osmium reaction systems.

Discussion

Apparently, the oxygen atom transfer reaction occurs with very small activation barrier (E_a) in the iridium reaction system but with very large E_a value in the osmium reaction system, as shown in Tables 1 and 2. These results are consistent with the experimental results that the reaction rapidly occurs in the iridium system but very slowly in the osmium system.

Table 3. Pendant Angles (θ)[a] of ML_n, $ML_n{=}O$, and Transition-State (M = Ir or Os; L = 2,4,6-trimethylphenyl for Ir and tris(2,6-diisopropylphenyl)imide for Os) and Reorganization Energies (E_{reorg}) (in kcal/mol)

	θ			E_{reorg}	
	ML_n	$ML_n{=}O$	TS	ML_n	$ML_n{=}O$
Ir	109.2	110.3	113.0	109.2	110.3
Os	90.9	108.0	100.8	90.9	108.0

[a] See Scheme 2 for the pendant angle.

It is worth elucidating the reasons why the significantly large difference is observed between the iridium and osmium systems in spite of their similar geometries and similar M=O bond energies.[25,26] Here, we make analyses by decomposing the E_a value into nuclear and electronic parts, like the discussion presented by Fortner and his co-workers.[25] To exchange an oxygen atom, ML_3 and $ML_3{=}O$ complexes have to change their geometries into those of TS. The destabilization energy induced by the geometry change corresponds to the reorganization energy in atom transfer event, which is considered as the nuclear factor. The electronic factor basically relates to the interaction between electron donor orbital of ML_3 and electron acceptor orbital of $ML_3{=}O$. Decrease of the reorganization energy and increase of the interaction lead to decrease of the activation barrier of the reaction.

Nuclear Factor. In various geometry changes, the largest change is observed at the pendent angle, definition of which is given in Scheme 2. This means that the pendant angle can be taken as reaction coordinate. We evaluated the reorganization energy as the energy difference of the reactant between the fully optimized geometry and the partially optimized one in which only the pendant angle was fixed to be the same as that of the transition state.

The reorganization energy of the osmium system is much larger than that of the iridium system, as shown in

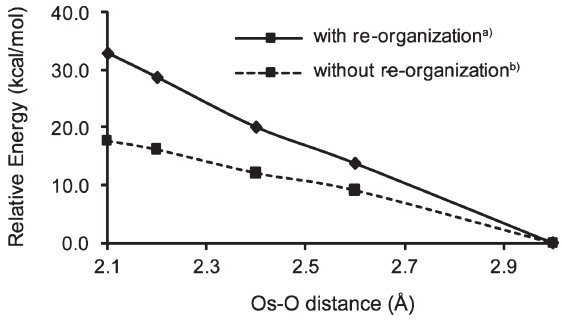

Figure 3. Potential energy curves against the Os−O distance in the Os system with and without reorganization energy. (a) The geometry was fully optimized except for the reaction coordinate, the Os−O distance. (b) Geometries of $\mathbf{Os(NAr)_3}$ and $\mathbf{Os(NAr)_3=O}$ were taken to be the same as those in the transition state.

Table 3; in particular, the reorganization energy of $\mathbf{Os(NAr)_3}$ is very large. This difference is easily interpreted in terms of the geometries of the reactant, transition state, and product. In the iridium system, $\mathbf{Ir(Mes)_3}$, $\mathbf{Ir(Mes)_3=O}$, and $\mathbf{TS_{IrMes}}$ all have tetrahedral-like structures around the Ir center, as shown in Figure 1, in which the pendant angle is similar to each other. As a result, the geometry change does not necessarily occur so much upon going from $\mathbf{Ir(Mes)_3}$ and $\mathbf{Ir(Mes)_3=O}$ to $\mathbf{TS_{IrMes}}$, leading to the small reorganization energy. In the osmium system, on the other hand, $\mathbf{Os(NAr)_3}$ is trigonal planar, as shown in Figure 2, but $\mathbf{TS_{Os}}$ and $\mathbf{Os(NAr)_3=O}$ have tetrahedral-like structure around the Os center. Thus, the structure of $\mathbf{Os(NAr)_3}$ considerably changes upon going to $\mathbf{TS_{Os}}$ from $\mathbf{Os(NAr)_3}$. This is the reason why the reorganization energy of $\mathbf{Os(NAr)_3}$ is considerably large.

To investigate how much the nuclear factor contributes to the activation barrier, the PEC without the reorganization energy was calculated in the osmium system, as shown in Figure 3, where one of the Os−O distances was taken as the reaction coordinate and the pendent angle was fixed to that of $\mathbf{TS_{Os}}$. This PEC still represents the activation barrier of about 10 kcal/mol, which is about 30% of the total activation barrier. Hence, it is concluded that the nuclear factor contributes to 70% of the activation barrier of the osmium reaction system and the electronic factor still contributes to 30% of the activation barrier.

The Reasons that the Geometry of $\mathbf{Os(NAr)_3}$ is Trigonal-Planar but That of $\mathbf{Ir(Mes)_3}$ is Tetrahedral-like. Because the large reorganization energy of $\mathbf{Os(NAr)_3}$ arises from its trigonal planar geometry and the small reorganization energy of $\mathbf{Ir(Mes)_3}$ arises from its tetrahedral-like geometry, as discussed above, it is worth investigating the reason why the geometry of $\mathbf{Ir(Mes)_3}$ is tetrahedral-like but that of $\mathbf{Os(NAr)_3}$ is trigonal planar. The frontier orbital energies of $\mathbf{Ir(Mes)_3}$ and $\mathbf{Os(NAr)_3}$ are shown in Schemes 3 and 4, respectively. Metal d orbitals play important role to construct these frontier orbitals, as follows: the HOMO (a_1) of $\mathbf{Ir(Mes)_3}$ mainly consists of the Ir d_{z^2} orbital. Because of the presence of the π orbitals of the mesityl ligand, π-type bonding and antibonding molecular orbitals (MOs) are formed in the HOMO−2 (2e) and the HOMO−1 (3e), respectively; indeed, the HOMO−1 largely consists of Ir d_π orbital into which

Scheme 3. Selected Molecular Orbitals of $\mathbf{Ir(Mes)_3}$ at Tetrahedral and Trigonal Planar Geometries[a]

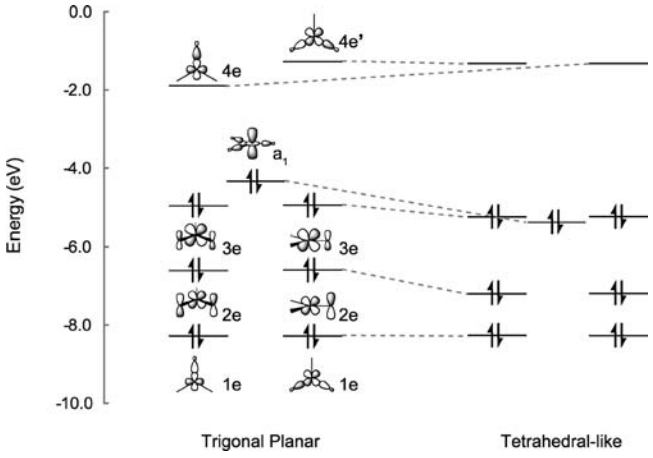

[a] The 4e and 4e′ orbitals are degenerate in model complex ($\mathbf{Ir(CH_3)_3}$). Splitting of these orbitals in $\mathbf{Ir(Mes)_3}$ is induced by the symmetry deviation of mesityl ligand.

the π orbital of the mesityl ligand mixes in an antibonding way. The HOMO−2 (2e) largely consists of the occupied π orbitals of the mesityl group into which the Ir d_π orbital mixes in a bonding way. Because the Ir(III) center has six d electrons, these $d_\pi-p_\pi$ bonding and antibonding orbitals are doubly occupied. The bonding orbital (HOMO−2) is stabilized by the geometry change to the tetrahedral-like structure from the planar one, because the overlap between the Ir d_π and the mesityl π orbitals increases by this geometry change, as shown in Scheme 3. Usually, the $d_\pi-p_\pi$ antibonding orbital energy rises when the $d_\pi-p_\pi$ bonding orbital energy becomes lower. However, the HOMO−1 energy becomes moderately lower by this geometry change, unexpectedly. This energy stabilization can be understood in terms of the mixing of the π^* orbital of the mesityl into the $d_\pi-\pi$ antibonding orbital; for detailed discussion see Supporting Information S3. The HOMO energy also decreases by this geometry change (Scheme 3). The reason is interpreted as follows: The HOMO involves antibonding interaction between the Ir d_{z^2} orbital and the mesityl sp^2 orbital. Because this antibonding interaction becomes weaker in the tetrahedral-like structure, the HOMO energy becomes lower by this geometry change. This is also important factor to stabilize the tetrahedral-like structure relative to the trigonal planar structure.

Though the MOs of $\mathbf{Os(NAr)_3}$ are similar to those of $\mathbf{Ir(Mes)_3}$, interesting differences in MO energy are observed between $\mathbf{Ir(Mes)_3}$ and $\mathbf{Os(NAr)_3}$, as shown in Schemes 3 and 4(A). Because the imide ligand has two doubly occupied π orbitals but no unoccupied π-type orbital, the imide forms strong π-donating interaction with the empty d_π orbitals of osmium, to raise the $d_\pi-p_\pi$ antibonding orbital energy; see the 3e MO in Scheme 4(A). As a result, the 3e MO energy becomes higher than the osmium d_{z^2} orbital energy. This is completely different from the $d_\pi-p_\pi$ antibonding orbital of the Ir complex, which is not destabilized very much because the mesityl group is not strongly π-donating. Also, the π^* orbital of the mesityl group participates in the π-type interaction to stabilize the iridium d_π orbital but the imide group does not have such π-type unoccupied orbital. Because the

Scheme 4. (A) Selected Molecular Orbitals of **Os(NAr)$_3$** at Tetrahedral-like and Trigonal Planar Geometries and (B) Important Molecular Orbitals of the Tetrahedral-like Geometry

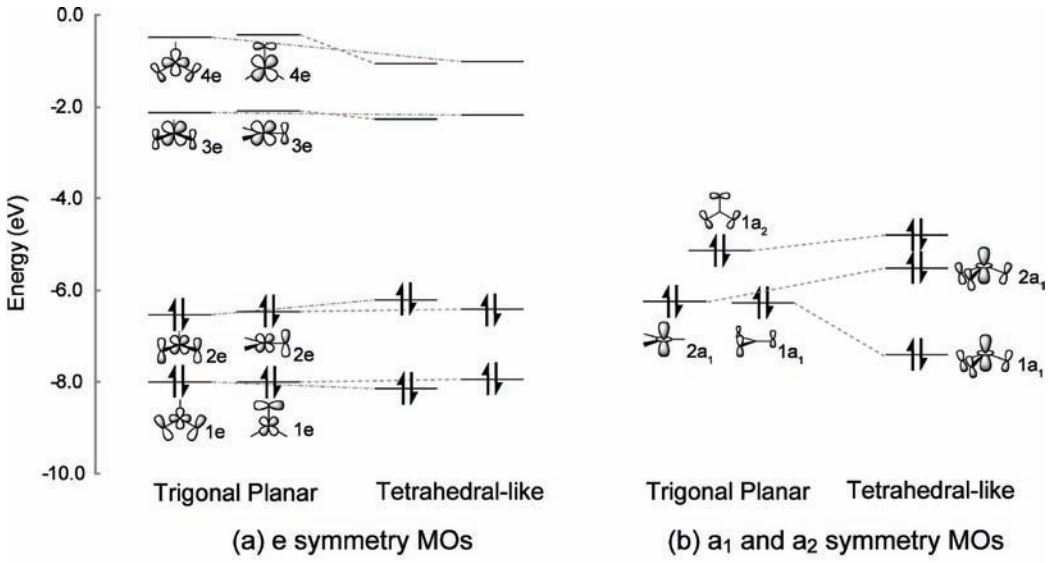

(A) Selected molecular orbitals of Os(NAr)$_3$ at tetrahedral-like and trigonal planar geometries

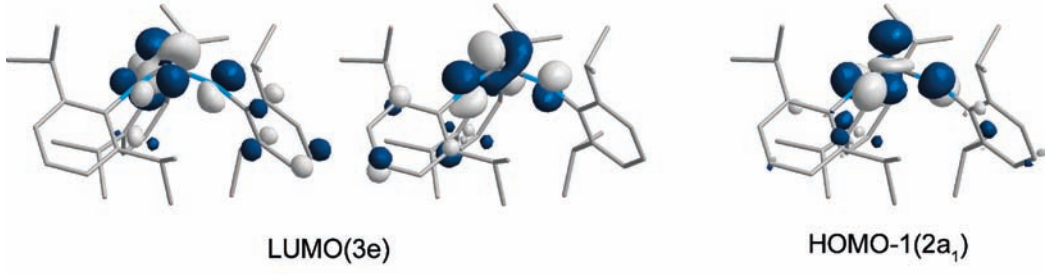

(B) Important molecular orbitals of the tetrahedral-like geometry

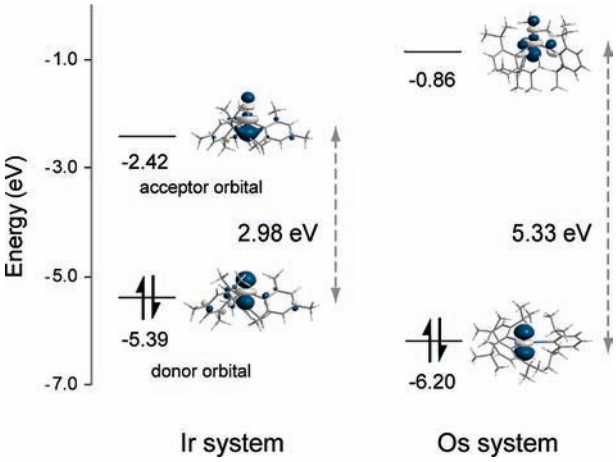

Figure 4. Electron donor orbitals of **Ir(Mes)$_3$** and **Os(NAr)$_3$** and acceptor orbitals of **Ir(Mes)$_3$=O** and **Os(NAr)$_3$=O**.

Os(VI) center has d^2 electron configuration, only the d_{z^2} orbital ($2a_1$) is doubly occupied and the π antibonding orbitals (3e) are unoccupied. This means that the $d_\pi - p_\pi$ antibonding orbital does not contribute at all to the energy stabilization of the tetrahedral-like structure unlike it in **Ir(Mes)$_3$**. It is noted that the HOMO−1 (d_{z^2}) energy rises by the geometry change to the tetrahedral-like structure, as shown in Scheme 4(A). This result is interpreted, as follows: Though the antibonding interaction between the osmium d_{z^2} orbital and the imide σ-orbital becomes weak by the geometry change, the antibonding interaction between the osmium d_{z^2} orbital and the imide π orbital is newly formed, as show in Scheme 4(B). In other words, four-electron repulsion newly occurs between doubly occupied d_{z^2} and imide π orbitals in the $2a_1$ MO of the tetrahedral-like structure. This four-electron repulsion is large because the imide is strongly π-electron donating. As a result, the net energy stabilization is not produced by the geometry change to the tetrahedral-like structure. Thus, the trigonal planar structure is more stable than the tetrahedral-like structure in **Os(NAr)$_3$**.

In conclusion, **Os(NAr)$_3$** has the trigonal planar structure because of the presence of the doubly occupied π orbitals of imide and the d^2 electron configuration of

Os(VI). This leads to the large reorganization energy of the osmium reaction system.

Electronic Factor. The electronic factor deeply relates to the interaction between wave functions of ML_3 and ML_3=O. Because the electron-deficient ML_n=O interacts with the electron-rich ML_n, the charge transfer (CT) occurs from ML_n to ML_n=O. Actually, the iridium and oxygen atomic populations of **Ir(Mes)$_3$=O** increase by 0.25 and 0.19 e, respectively, upon going to **TS$_{IrMes}$**, but the iridium atomic population of **Ir(Mes)$_3$** decreases by 0.23 e, where Mulliken population analysis was employed. The osmium and oxygen atomic populations of **Os(NAr)$_3$=O** increase by 0.13 and 0.08 e, respectively, while the osmium atomic population of **Os(NAr)$_3$** decreases by 0.34 e upon going to **TS$_{Os}$**. In this CT interaction, the σ-type acceptor orbital of ML_3=O and the σ-type donor orbital of ML_3 play important role, because the M−O−M is almost linear in the transition state. The iridium and osmium complexes possess the similar σ-type occupied and unoccupied orbitals along z-axis, as shown in Figure 4. This means that the donor orbital overlaps with the acceptor orbital in a similar extent between iridium and osmium systems. However, the energy gap between the donor and the acceptor orbitals is much smaller in the iridium complex than in the osmium complex (Figure 4). Because of this small energy gap in the iridium system, strong CT interaction is formed between **Ir(Mes)$_3$=O** and **Ir(Mes)$_3$**, which leads to the large electronic factor. In the osmium system, on the other hand, the CT interaction between **Os(NAr)$_3$=O** and **Os(NAr)$_3$** is considerably weak because of the large energy gap, which leads to the small electronic factor.

We calculated ionization potentials (IPs) of **Ir(CH$_3$)$_3$** and **Os(NCH$_3$)$_3$** and the electron affinities (EAs) of **Ir(CH$_3$)$_3$=O** and **Os(NCH$_3$)$_3$=O**. The IP of **Os(NCH$_3$)$_3$** is larger than that of **Ir(CH$_3$)$_3$** by 0.27 eV, and the EA of Os(NCH$_3$)$_3$=O is smaller than that of **Ir(CH$_3$)$_3$=O** by 0.24 eV. These results also suggest that the CT interaction occurs much easier in the iridium system than in the osmium system.[42]

The next issue to be discussed is the reason why the energy gap is large in the osmium system. This large energy gap of the osmium reaction system arises from the fact that the acceptor orbital of **Os(NAr)$_3$=O** exists at higher energy and the donor orbital of **Os(NAr)$_3$** exists at lower energy than those of **Ir(Mes)$_3$=O** and **Ir(Mes)$_3$**, respectively; see Figure 4. The acceptor orbital of **Os(NAr)$_3$=O** involves the quasi d_{z^2}-p antibonding overlap between the osmium d_{z^2} and nitrogen p orbitals (Figure 4), as proposed in a previous study.[25] As discussed above, this antibonding interaction arises from the presence of the doubly occupied p_π orbitals of the imide group; in other words, the doubly occupied p_π orbitals of the imide group raises the σ-type acceptor orbital energy of **Os(NAr)$_3$=O** through the d_{z^2}-p antibonding overlap to decrease the electronic factor. In **Ir(Mes)$_3$=O**, such antibonding interaction is not involved in the σ-type acceptor orbital because the mesityl group does not possess strongly π-donating orbital, as discussed above. As a result, the acceptor orbital of **Ir(Mes)$_3$=O** is not destabilized very much.

The donor orbital of **Ir(Mes)$_3$** mainly consists of Ir d_{z^2} orbital into which the sp^2 orbital of mesityl ligand moderately mixes in antibonding way. On the other hand, the donor orbital of **Os(NAr)$_3$** consists of the Os d_{z^2} orbital without any orbital mixing of ligand. Moreover, the osmium center takes +6 oxidation state, while the iridium center takes +3 oxidation state. As a result, the donor orbital of **Os(NAr)$_3$** is at lower energy than that of **Ir(Mes)$_3$**.

Conclusions

The oxygen atom transfer reactions of iridium and osmium complexes were theoretically investigated with the DFT method. In small model systems, in which bulky substituents were replaced with methyl groups, the μ-oxo dinuclear iridium and osmium complexes were optimized as stable species, indicating that the oxygen atom transfer reaction does not occur in model systems. In real systems, on the other hand, the transition states of both iridium and osmium reactions were successfully optimized. It is noted here that the transition state is unsymmetrical in the iridium system but symmetrical in the osmium system. Interestingly, symmetrical μ-oxo bridged dinuclear intermediate was optimized in the iridium system, geometry of which agrees well with experimental one. Besides the transition states and the symmetrical intermediate, unsymmetrical intermediate was newly optimized in the iridium system, while no intermediate was optimized in the osmium system.

The activation barrier in gas phase is calculated to be 3.9 and 33.3 kcal/mol for the iridium and osmium reaction systems, respectively, in the potential energy surface.[40] The $\Delta G^{0\ddagger}$ value is evaluated to be 8.8 and 43.8 kcal/mol for the iridium and osmium reaction systems, respectively, in solution at 298.15 K. These results are consistent with experimental results that the oxygen atom transfer reaction rapidly occurs in the iridium system but very slowly in the osmium system.[25]

The origin of the large difference in the activation barrier is discussed in terms of nuclear and electronic factors. The nuclear factor arises from reorganization energy, which is defined as the destabilization energy necessary to distort the reactant from the equilibrium structure into the transition state structure. The nuclear factor is much larger in the osmium system than in the iridium system. In the osmium reaction system, the activation barrier without reorganization energy is about 70% of the total activation barrier, indicating that the nuclear factor largely contributes to the difference in the reactivity between the iridium and osmium complexes but the electronic factor also contributes to the difference. The larger nuclear factor of osmium system arises

(42) In **IrMe$_3$** and **Os(NMe)$_3$**, the σ-type donor orbitals are HOMO, and in **IrMe$_3$=O** and **Os(NMe)$_3$=O**, the σ*-type acceptor orbitals are LUMO. We evaluated the IPs of the former HOMOs and the EAs of the latter LUMOs with the DFT/BS-II and CCSD(T)/BS-II; see Supporting Information Table S4. We also tried to evaluate the IPs of the σ-type donor orbitals of **Ir(Mes)$_3$** and **Os(NAr)$_3$**, but failed it; though we started the SCF calculation with the singly occupied σ-type donor orbital, the π-orbital became singly occupied and the σ-type donor orbital became doubly occupied during the SCF calculation. This is because the HOMOs of **Ir(Mes)$_3$** and **Os(NAr)$_3$** are the π orbital of the ligand. Also, we tried to evaluate the EAs of the σ-type acceptor orbitals of **Ir(Mes)$_3$=O** and **Os(NAr)$_3$=O**, but failed it: The π* orbital of the ligand became the singly occupied and the σ*-type acceptor orbital became unoccupied during the SCF calculation, even though we started the SCF calculation with the singly occupied σ*-type acceptor orbital. Thus, we presented discussion based on the IPs and EAs of model systems.

from the fact that substantially large structural changes must occur upon going from trigonal planar $\mathbf{Os(NAr)_3}$ to the tetrahedral-like transition state. The small reorganization energy of the iridium system arises from the fact that structural change little occurs upon going from $\mathbf{IM_{IrMes}}$ to $\mathbf{TS_{IrMes}}$ because $\mathbf{Ir(Mes)_3}$, $\mathbf{Ir(Mes)_3=O}$, $\mathbf{TS_{IrMes}}$, and $\mathbf{IM_{IrMes}}$ all take tetrahedral-like structure around the iridium center.

The electronic factor was discussed in terms of the interaction between the donor orbital of ML_3 and the acceptor orbital of ML_3=O. Since the donor and acceptor orbitals are similar between the iridium and osmium complexes, it is likely that the extent of orbital overlap is similar between these two systems. However, the energy gap between the donor and acceptor orbitals is much larger in the osmium reaction system than in the iridium reaction system, which leads to the smaller electronic factor in the osmium system than in the iridium system. The large energy gap in the osmium system arises from both the electron donor and electron acceptor orbitals; the electron donor orbital of $\mathbf{Os(NAr)_3}$ is at much lower energy than that of $\mathbf{Ir(Mes)_3}$ since osmium center takes +6 oxidation state while iridium center takes +3 oxidation state. Similarly, the electron acceptor orbital of $\mathbf{Os(NAr)_3=O}$ is at much high energy than that of $\mathbf{Ir(Mes)_3=O}$ because of the quasi-d_{z^2}-p antibonding overlap between the osmium d_{z^2} and nitrogen p orbitals.

Acknowledgment. This work was financially supported by Grand-in-Aids on basis research (No. 1530012), Priority Areas for "Molecular Theory for Real Systems" (No. 461), and NAREGI Project from the Ministry of Education, Science, Sports, and Culture. Some of theoretical calculations were performed with SGI workstations of Institute for Molecular Science (Okazaki, Japan), and some of them were carried out with PC cluster computers in our laboratory.

Supporting Information Available: Detailed discussion about Scheme 3, procedure for the evaluation of the translational entropy in solution, Cartesian coordinates of optimized geometry of $\mathbf{Ir(Mes)_3}$, $\mathbf{Ir(Mes)_3=O}$, $\mathbf{IM_{IrMes}}$, $\mathbf{Os(NAr)_3}$, $\mathbf{Os(NAr)_3=O}$, $\mathbf{TS_{Os}}$, electronic energies of iridium and osmium model and real systems in singlet and triplet states, calculated Ir=O and Os=O bond energies (kcal/mol) in $\mathbf{Ir(CH_3)_3=O}$ and $\mathbf{Os(NCH_3)_3=O}$ complexes, optimized geometry of $\mathbf{Ir(Ph)_3-O-Ir(Ph)_3}$, andpotential energy curves against the Ir−O−Ir angle in $\mathbf{Ir(Ph)_3-O-Ir(Ph)_3}$. This material is available free of charge via the Internet at http://pubs.acs.org.